



# IJSRM

INTERNATIONAL JOURNAL OF SCIENCE AND RESEARCH METHODOLOGY

An Official Publication of Human Journals



Human Journals

Research Article

February 2018 Vol.:8, Issue:4

© All rights are reserved by Mona A. El Naggar

## Mathematical Investigation on EMF Thermal and Non-Thermal Effects on Arteries with Implants: LF and HF Exposure



**IJSRM**  
INTERNATIONAL JOURNAL OF SCIENCE AND RESEARCH METHODOLOGY  
An Official Publication of Human Journals



**Mona A. El Naggar**

*Engineering Math. & Physics Dept., Faculty of Engineering, Cairo University, Cairo, Egypt*

**Submission:** 24 January 2018  
**Accepted:** 29 January 2018  
**Published:** 28 February 2018



HUMAN JOURNALS

[www.ijsrm.humanjournals.com](http://www.ijsrm.humanjournals.com)

**Keywords:** Far field exposure, Mathematical model, Dissipated and stored power density, Arterial implants, Silicone rubber stents, LF exposure, HF exposure.

### ABSTRACT

The present work investigates the electromagnetic power absorbed in arteries and blood due to far field exposure. A mathematical model is adopted to trace the electromagnetic field penetration, covering the low frequency range, LF (30kHz -300kHz), and the high frequency range, HF (3MHz-900MHz), through an artery with implanted stent. The model calculates the dissipated and stored power density due to the EMF far field exposure. The frequency dependence of thermal and non-thermal effects on the artery and on the flowing blood is hence assessed. The proposed model compares the power density distribution with frequency in the absence and the presence of the implant. The thermal and non-thermal effects due to dissipated power density and that stored respectively are hence estimated within electric field strengths (1V/m-1kV/m).

## 1. INTRODUCTION

EMF exposure has recently become an essential research field due to the constantly increasing dependence on microwave, UHF, VHF and other frequency ranges serving various technology applications. Scientists are concerned with assessing the EMF biological effects.[1-4] The effect of human EMF exposure is usually assessed by either whole or partial body measurements. These measurements assess the amount of EMF energy absorbed due to near or far field exposure by phantom models [5-6] and computer simulation and numerical analysis techniques [7-10]. Mathematical modeling of EMF energy absorption in biological tissues and systems is an important method of this assessment [11 -14]. International standardization establishments issue Maximum Permissible Exposure (MPE) levels for humans, partial and whole body, regularly. These MPE levels are expressed in terms of maximum electric or magnetic field strength, Specific Absorption Rate (SAR), or power density absorbed in the biological tissue [15-17], specifying neither tissue or organ type nor issuing special limits for patients with implanted medical devices. Standards for safety levels of human exposure to EMF of frequency ranges; (0–3 kHz) [18] and (3 kHz -3GHz) [17-19] are issued and updated periodically. These institutional standards mostly indicate thermal effects in terms of the absorption rates reported, whereas non-thermal effects are not yet addressed by these institutes. Researchers investigate the non-thermal effect of the EMF as either interaction with ionic fluids [20] or as the power stored in a specific body tissue [21].

Vascular substitutes or stents, used for the treatment of arterial blockage, usually made of stainless steel, exhibit compliance mismatch. A *silicone- silicone rubber stent* section was introduced and compared to the commonly used stainless steel stent [22]. The present work investigates the *silicone rubber stent* response to EMF exposure by comparing the induced power in an arterial section and blood inside in two cases, with and without a stent implant.

The present work aims to employ an analytical approach to calculate the average power density absorbed, both stored and dissipated, within a cylindrical section of an artery of diameter 12mm and thickness 3mm, with blood inside. The proposed model assumes the normal incidence of a vertically polarized electromagnetic wave, of field strength range (1V/m-1kV/m), to be incident on the arterial section in two cases: an arterial section without stent and another with a silicone rubber stent implant. In each case, the power density, dissipated and stored, is computed for the artery and for the blood. Hence, the computed results are investigated to estimate the thermal and non-thermal effects resulting from far

field exposure in the *LF* and in the *HF* ranges. These ranges are divided according to the international standards as LF (30kHz-300kHz), HF (3MHz-900MHz).

The present work compares arterial response to the specified *EMF* far field exposure in two cases; without a stent implant and with a *silicone rubber* one. Besides being biocompatible, mechanically compatible, the *silicone rubber* is a recommended material for stent manufacture.

## 2. MATHEMATICAL MODEL

The mathematical model considers two cases namely, the *EMF* exposure of an arterial section with flowing blood. Secondly, the exposure when the artery is provided with an implanted stent. The equations governing the total electric and magnetic field distributions in each layer are deduced, considering the respective biological electromagnetic properties. MapleV computer programming is adopted. The values of real and imaginary components of the *EMF* power densities are computed as a function of frequency and electric field strength. Maxwell's equations are employed using the reported electromagnetic properties of arteries and blood [23-25]. The model assumes the incidence of a polarized electromagnetic wave on a homogeneous arterial section where a sample of  $1\text{mm}^2$  surface area is studied. The reflection on successive interfaces contributes to the overall calculated power. The electromagnetic properties such as permittivity,  $\epsilon(f)$ , conductivity,  $\sigma(f)$ , and permeability,  $\mu(f)$  of each medium are inserted in the model, as complex functions of frequency. The average power density for the frequency range (1kHz-100MHz) and the electric field strengths (1V/m-1KV/m), is calculated for the artery, the stent and the blood. The average power density,  $P_{av}$ , is calculated as a complex function of  $f$  and  $E_0$ :

$$P_{av} = \frac{1}{\Delta x} \int_0^{\Delta x} \frac{1}{T} \sqrt{\left\{ \int_0^T \{P_x(x,t)\}^2 dt \right\}} dx \quad (1)$$

where:  $P_x(x,t) = E_y(x,t) \times H_z(x,t)$ ,  $T=1/f$ ,  $f$  is the incident *EMF* frequency and  $\Delta x$  is the direction of the wave propagation into the layer thickness  $\Delta x$ . The dissipated power density,  $P_{diss}$ , and that stored,  $P_{str}$ , are the real and imaginary components of  $P_{av}$ . Appendix 1 shows detailed mathematical analysis.

### 3. RESULTS

A far field *EMF* exposure is assumed to be normally incident on the outer layer of an arterial cylindrical section with blood inside. The dissipated power density,  $P_{diss}$ , and that stored,  $P_{str}$ , are calculated in ( $w/m^2$ ), for different values of field strengths,  $E_0$ , in each layer for the two abovementioned *cases*.

For the first case, figures (1a, 1b) illustrate the power densities  $P_{diss}$  and  $P_{str}$ , respectively versus the frequency,  $f$ , in an arterial section without a stent implant, in the range (1kHz-800kHz). Figures (2a, 2b) show these power density distributions versus  $f$ , in blood for the same *LF range*. Whereas, figures (3-a, 3-b) show the power density distributions in the arterial section, in the range (1MHz-200MHz). Figures (4-a,4-b) show the distributions of these power densities in blood for the same *HF range* as well.

For the second case, at *LF* figures (5-a, 5-b) show  $P_{diss}$  and  $P_{str}$ , in an arterial section with a silicone rubber stent implant, versus  $f$ . Whereas figures (6-a, 6-b) show these power density distributions for the blood inside it.

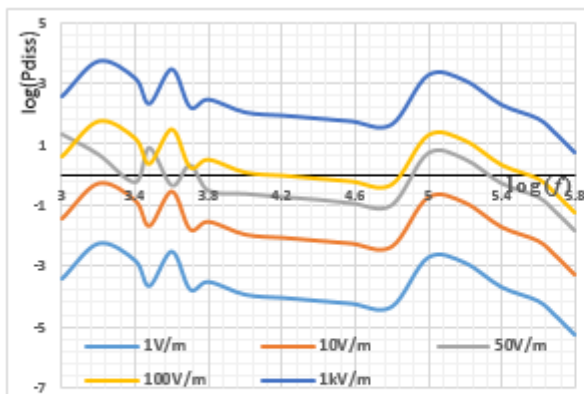


Fig.1-a Dissipated power density within an artery without stent  $\log(P_{diss})$  vs  $\log(f)$  LF range

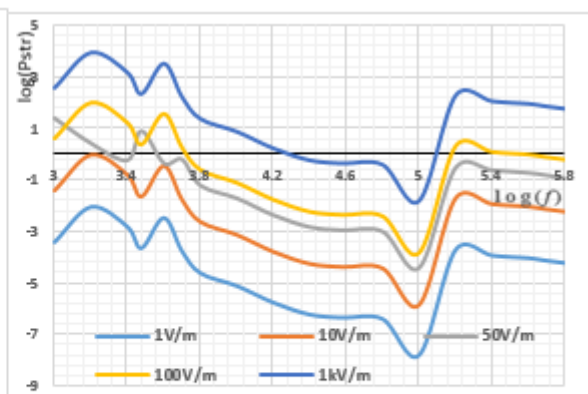


Fig.1-b Stored power density within an artery without stent  $\log(P_{str})$  vs  $\log(f)$  LF range

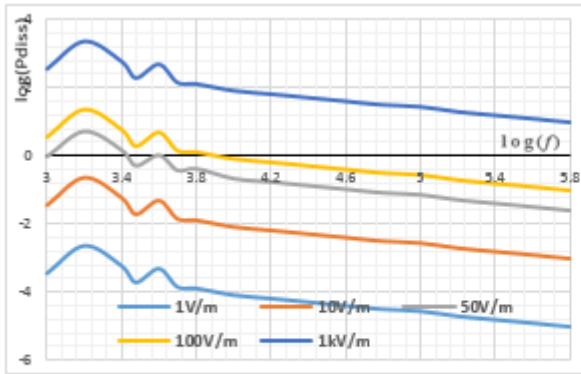


Fig. 2-a Dissipated power density in blood within an artery without stent  $\log(P_{diss})$  vs  $\log(f)$  LF range

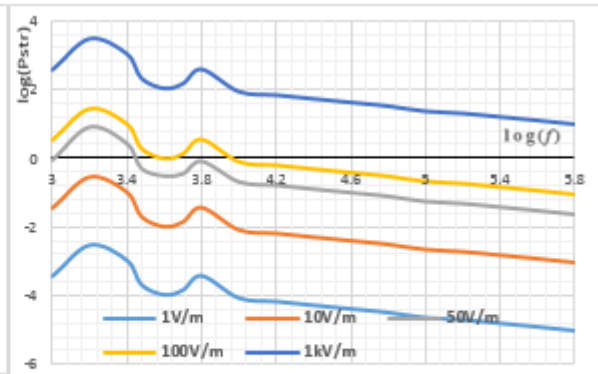


Fig. 2-b Stored power density in blood within an artery without stent  $\log(P_{str})$  vs  $\log(f)$  LF range

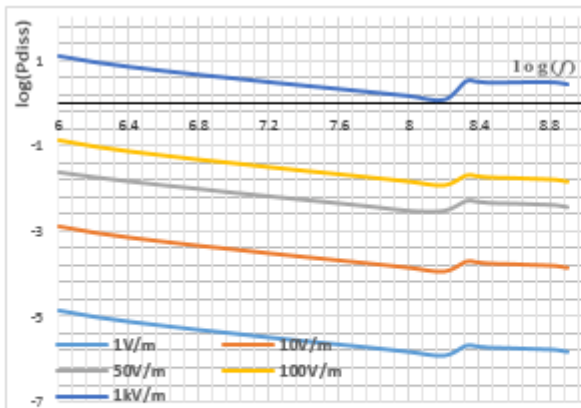


Fig. 3-a Dissipated power density within an artery without stent  $\log(P_{diss})$  vs  $\log(f)$  HF range

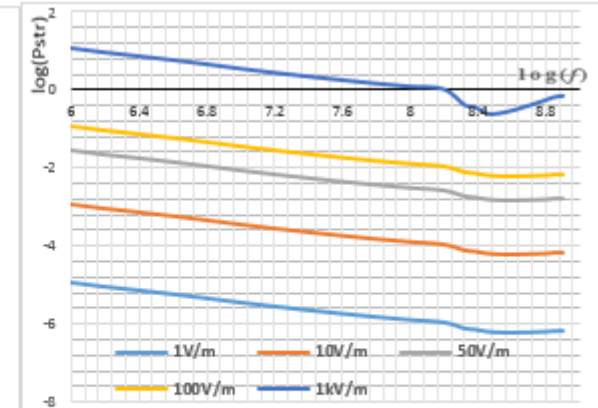


Fig. 3-b Stored power density within an artery without stent  $\log(P_{str})$  vs  $\log(f)$  HF range

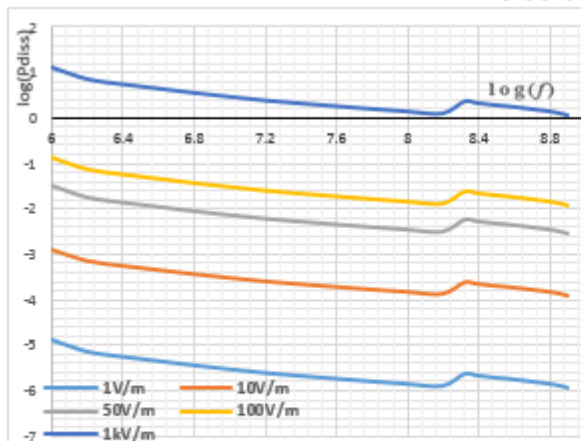


Fig. 4-a Dissipated power density in blood within an artery without stent  $\log(P_{diss})$  vs  $\log(f)$  HF range

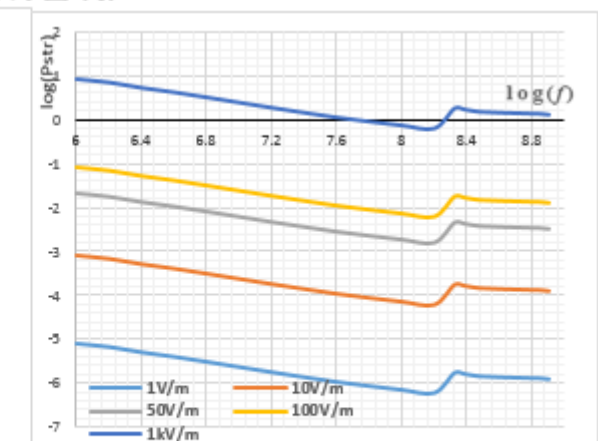


Fig. 4-b Stored power density in blood within an artery without stent  $\log(P_{str})$  vs  $\log(f)$  HF range

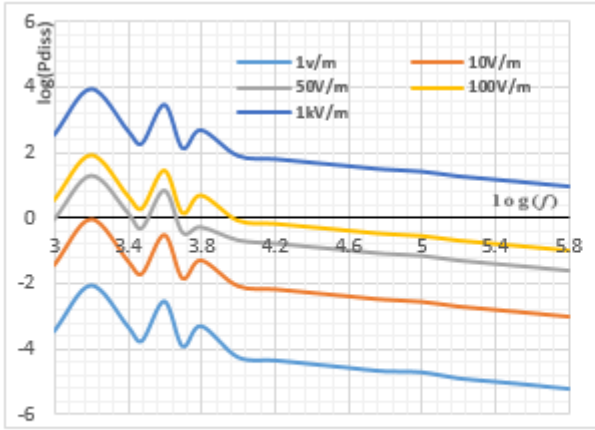


Fig.5-a Dissipated power density within an artery with silicone rubber stent  $\log(P_{diss})$  vs  $\log(f)$  LF range

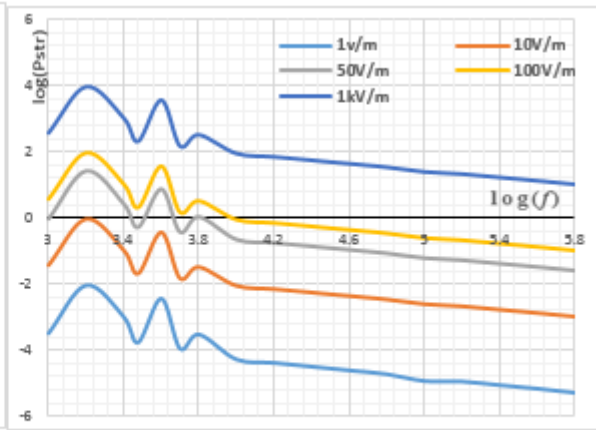


Fig.5-b Stored power density within an artery with silicone rubber stent  $\log(P_{str})$  vs  $\log(f)$  LF range

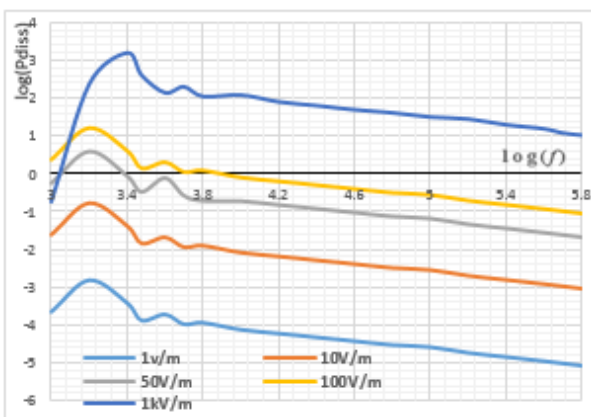


Fig.6-a Dissipated power density in blood within an artery with silicone rubber stent  $\log(P_{diss})$  vs  $\log(f)$  LF range

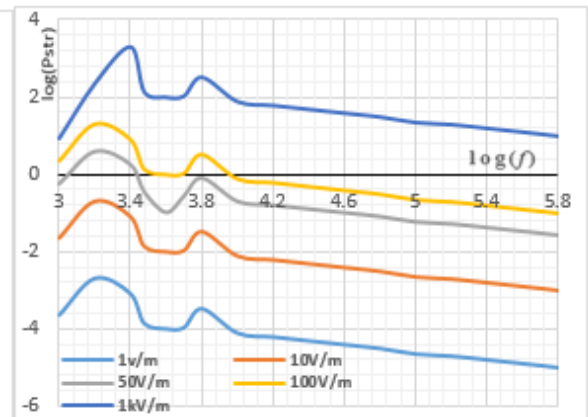


Fig.6-b Stored power density in blood within an artery with silicone rubber stent  $\log(P_{str})$  vs  $\log(f)$  LF range

While figures (7-a,7-b) show these distributions in the arterial section, in the range (1MHz-900MHz). Figures (8-a,8-b) show the power densities for blood at HF.

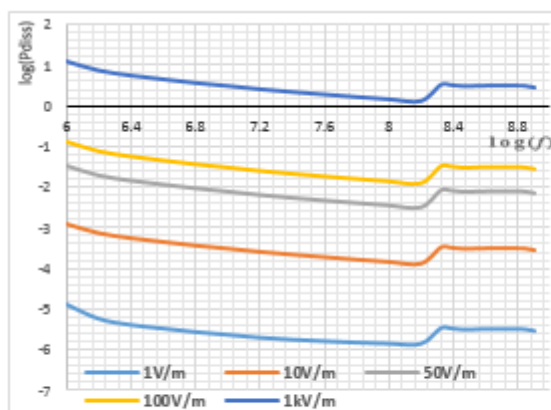


Fig.7-a Dissipated power density within an artery with silicone rubber stent  $\log(P_{diss})$  vs  $\log(f)$  HF range

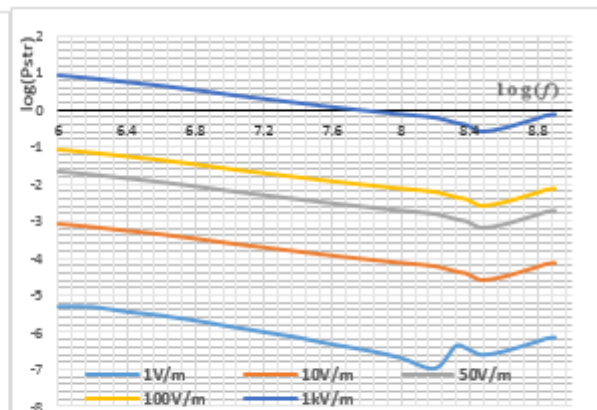


Fig.7-b Stored power density within an artery with silicone rubber stent  $\log(P_{str})$  vs  $\log(f)$  HF range

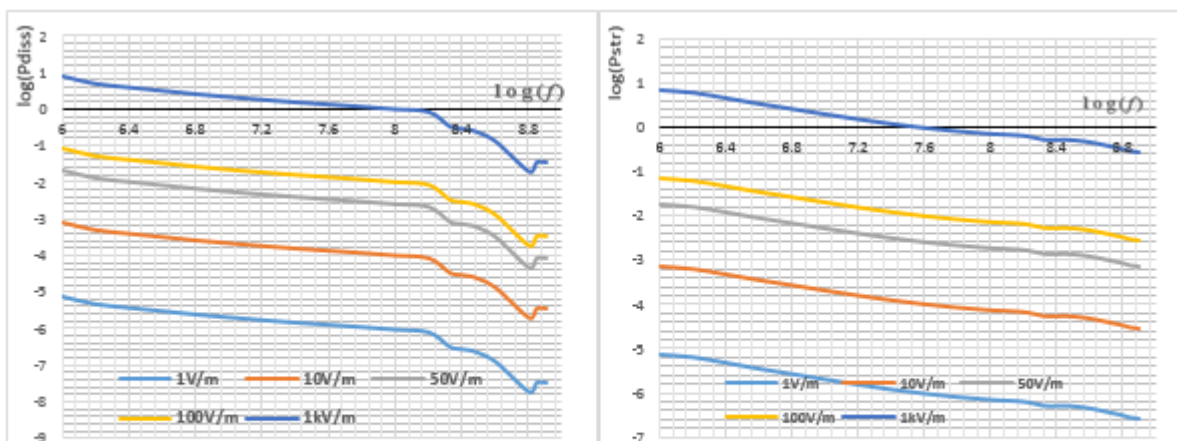


Fig.8-a Dissipated power density in blood within an artery with silicone rubber stent  $\log(P_{diss})$  vs  $\log(f)$  HF range

Fig.8-b Stored power density in blood within an artery with silicone rubber stent  $\log(P_{str})$  vs  $\log(f)$  HF range

#### 4. DISCUSSION

The frequency range, (1kHz-800kHz), covers the traditional *LF* range while the range (1MHz-900MHz) covers the *HF* one. These two ranges are chosen to match most of the EMF applications including medical diagnosis and treatment. The electric field exposure is taken to comply with the average values emitted by these sources (1V/m-1kV/m). The present work considers the complex nature of the permittivity and its frequency dependence. Hence the dissipated and stored powers are highly dependent on this physical property. However, the measurements of the biological tissue permittivity are subject to a considerable inconsistency which may affect the final results thus accounts for the fluctuations appearing on *LF* figures.

#### 5. CONCLUSION

The present results indicate that for *LF* exposure, at  $E_0 \geq 1kV/m$ , the incident EMF induces thermal and non-thermal effects that exceed the *LF* safety standards [16] [19] [26]. Whereas, Table 1 illustrates a comparison for *HF* exposure with the international MPE. For  $E_0 = 1kV/m$  the power density is higher than *HF* safety standards only at the shown frequencies.

Since the power penetration depends on the thickness of the considered layers, the preliminary work showed that the skin effect for both artery and stent is insignificant, as far as the power dissipated or stored is concerned.

The dissipated power density is considered the main source of thermal effect. Traditionally, *stainless steel*, which is commonly used for stent implants in arteries, may screen the blood from any power exposure. On the other hand, it reflects most of the power back to the artery

causing a considerable temperature rise. *Silicone rubber* is not only highly compatible but also enjoys better mechanical properties. The present work confirms that this material is capable of distributing the incident energy between the blood and the artery. Accordingly, lower *thermal* effects result compared to those induced by *metallic* stents.

Caution should be given when people are exposed to *LF* at electric fields exceeding or equal to 1kV/m. Since above this field strength, the absorbed power exceeds the MPE levels.

Particular concern should be given for the people with implants when they are subjected to medical devices that utilize *HF* apparatus.

**Table 1 HF Exposure**

MPE Level (W/m <sup>2</sup> )	f (MHz)	E <sub>0</sub> =1kV/m							
		Present Work(W/m <sup>2</sup> ) Artery				Present Work(W/m <sup>2</sup> ) Blood			
		without stent		with stent		without stent		with stent	
		P <sub>diss</sub>	P <sub>str</sub>	P <sub>diss</sub>	P <sub>str</sub>	P <sub>diss</sub>	P <sub>str</sub>	P <sub>diss</sub>	P <sub>str</sub>
ICNIRP [15] [16] IEEE [17] [18] [26] 300kHz-3GHz (Public:4.5W/ m <sup>2</sup> ) Occupational: (10W/m <sup>2</sup> )	1	13.294	11.45807	13.011	8.1215	13.2	7.96	7.9	7.02
	1.590	9.55	8.92255	7.592	6.669	7.29	6.69	4.86	6.12
	2.510	7.355	7.17508	5.666	5.3095	5.609	5.063	3.872	4.604
	3.980	5.87	5.733975	4.5499	4.2335	4.531	4.013	---	----
	6.310	4.735	4.4891	3.68285	-----	-----	----	----	----
	10	3.895	3.46986	-----	-----	----	----	----	----

**COMPETING INTERESTS**

“Authors have declared that no competing interests exist.”

**REFERENCES**

- [1] Stuchly M. A., " Fundamentals of the Interactions of Radio-frequency and Microwave Energies with Matter. Biological effects and dosimetry of nonionizing radiation, RF and microwave energies," *NATO advanced study institutes series*, Vols. Plenum Press, NY, 1983.
- [2] Repacholi M. H., "Low-Level Exposure to Radiofrequency Electromagnetic Fields:," *Health Effects and Research Needs. Bioelectromagnetics*, vol. (19) , p. 1–19, 1998.
- [3] Prisco M. G., Nasta F., Rosado M. M., Lovisolio G. A., Marino C., Pioli C., " Effects of GSM-modulated radiofrequency electromagnetic fields on mouse bone marrow cells," *Radiat Res.*, Vols. doi: 10.1667/RR1213.1, 170, no. (6), pp. 803-810., Dec 2008.
- [4] Gosselin M., C. Joseph W., et. al., " Estimation Formulas for the Specific Absorption Rate in Humans Exposed to Base-Station Antennas," *IEEE Transactions on Electromagnetic Compatibility*, 2011.
- [5] Yusoff N.I.M, Khatun S., Alshehri S.A., "Characterization of absorption loss for UWB body tissue propagation model," *Proceedings of the 2009 IEEE 9th Malaysia International Conference on*

Communications, 2009.

- [6] Christ A., Klingenbock A., Samaras T., Goiceanu C. and Kuster N, "The Dependence of Electromagnetic Far-Field Absorption on Body Tissue Composition in the Frequency Range from 300MHz to 6GHz.," *IEEE Transactions on microwave theory and techniques*, vol. 54.
- [7] Buleandra A., Petrescu T., "Comparison of specific absorption rates induced in a model of the human skull," *U.P.B. Sci.Bull.U.P.B. Sci.Bull.*, Vols. X (73), no. 1, pp. 83-92, 2011.
- [8] Foster R., "Thermal and Non-thermal Mechanisms of Interaction of Radio-Frequency Energy with Biological Systems," *IEEE Transactions on Plasma Science*, vol. 28, no. 1, Feb 2000.
- [9] Findlay R., "Computational Dosimetry and the EMF Directive A presentation for the Health & Safety. World Health Organization," *2013EMFComp*, vol. ISBN 924, 2006.
- [10] Jaime A. Ramirez, Dalmy F. Carvalho Jr, Elson J. Silva, "Determination of the temperature increase in the human eye due to electromagnetic fields," *COMPEL: The International Journal for Computation and Mathematics in Electrical and Electronic Engineering*, vol. 34, no. 5, pp. 1489-1500, <https://doi.org/10.1108/COMPEL-02-2015-0100>, 2015.
- [11] Gajšek P. D'Andrea J. A. Mason P. A. Zirix J. M. Walters T. J. Hurt W. D Meyer F. J. C. Jakobus U. Samaras T. Sahalos J. N., "Mathematical Modeling of EMF Energy Absorption in Biological Systems," *Biological Effects of Electromagnetic Fields*, vol. 11, 2003.
- [12] El Naggar M. A., "EMF Power Absorption in Bone and Bone Marrow: Mathematical Model," *Articleno.PSIJ2015.053, SCIENCE-DOMAIN international, www.sciencedomain.org*, vol. 7, no. 2348-0130, pp. 11-19, 2015.
- [13] El Naggar M. A., El Messierey M. A., "Evaluation of power absorption in human eye tissue," *International Journal of Advanced Research*, <http://www.journalijar.com>, vol. 1, no. Issue 7, ISSN 2320-5407, pp. 658-665, 2013.
- [14] Vecchia P., "Exposure of humans to electromagnetic fields," *Standards and regulations Ann Ist Super Sanità*, vol. 43, no. 3, pp. 260-267, 2007.
- [15] "ICNIRP guidelines for limiting exposure to time-varying electric, magnetic and electromagnetic fields (up to 300 GHz)," *Health Physics*, vol. 74, no. 4, p. 494-522, 1998.
- [16] ICNIRP publication, "International commission on non-ionizing radiation protection ICNIRP statement on the: Guidelines for limiting exposure to Time-varying electric, magnetic, and Electromagnetic fields (up to 300 GHz)," *Health Physics*, vol. 97, no. 3, p. 257-258., 2009.
- [17] S. b. t. I. I. Committee, "IEEE Standard for Safety Levels with Respect to Human Exposure to Radio Frequency Electromagnetic Fields, 3 kHz to 300 GHz.," I E E E 3 Park Avenue New York, NY 10016-5997, USA, Oct. 6 2009.
- [18] IEEE Standards, "C95.6TM IEEE Standard for Safety Levels with Respect to Human Exposure to Electromagnetic Fields, 0-3 kHz," The Institute of Electrical and Electronics Engineers, Inc. 3 Park Avenue, New York, NY 10016-5997, USA, 23 October 2002.
- [19] IEEE International Committee on Electromagnetic Safety(SCC39), "IEEE Standard for Safety Levels with Respect to Human Exposure to Radio Frequency Electromagnetic Fields, 3 kHz to 300 GHz," IEEE Std C95.1™, Park Avenue New York, NY 10016-5997, USA, 2005 (Revision of IEEE Std C95.1-1991).
- [20] El Naggar M. A., El Messierey M. A., "A Mathematical Model for Pulsating Flow of Ionic Fluid under an Axial Electric Field: EMF Effect on Blood Flow," *Journal of Physical Science and Application, JSAP*, vol. 2, no. ISSN 4, pp. 61-70, 2012.
- [21] Mona A. El Naggar, Medhat A. El-Messierey, "Thermal and Non-Thermal Microwave Absorption in Long Bone," *Ijsrm.Human Journals Research Article*, vol. 5, no. 1, pp. 102-111,[srm.humanjournals.com](http://srm.humanjournals.com), 2016.
- [22] Mona A. El-Naggar, "An Investigation on Silicone and Silicone Rubber Stents in Comparison with Stainless Steel Stents: Introducing a Double Layer Stent Model," *British Journal of Applied Science & Technology, science domain international, www.sciencedomain.org*, vol. 4, no. 15, ISSN: 2231-0843, pp. 2206-2222, May 2014.

- [23] L. R. G. C. Gabriel S., " The dielectric properties of biological tissues: Measurement in the frequency range 10Hz to 20GHz.," *Physics in medicine and biology*, vol. 41, no. 11, pp. 2251-2269, 1996.
- [24] G. C. G. S., " Compilation of the dielectric properties of body tissues at RF and microwave frequencies," Dielectric properties of the body tissues, June 1996.
- [25] N. Cararra, "An internet resource for the calculation of the dielectric properties of biological tissues in the frequency range of 10 Hz to 100 GHz.," <http://niremf.ifac.cnr.it/tissprop>.
- [26] S. C. C. 2. IEEE-SA Standards Board, "Standard for safety levels with respect to human exposure to electromagnetic fields, (0–3 kHz)," Sponsor IEEE International Committee on Electromagnetic Safety on Non-Ionizing Radiation, Approved 12 September 2002, Reaffirmed 5 December 2007.

**APPENDIX 1**

Reflection and transmission coefficients for the  $i^{th}$  layer are:

$$r_{hi}(f) = \frac{\sqrt{\varepsilon_{i+1}(f)} / \sqrt{\varepsilon_i(f)} - \cos\theta_{i+1} / \cos\theta_i}{\sqrt{\varepsilon_{i+1}(f)} / \sqrt{\varepsilon_i(f)} + \cos\theta_{i+1} / \cos\theta_i} \quad t_{h(i-1)}(f) = \frac{2}{\sqrt{\varepsilon_i(f)} / \sqrt{\varepsilon_{i-1}(f)} + \cos\theta_i / \cos\theta_{i-1}} \quad (1)$$

$$r_{vi}(f) = \frac{1 - \sqrt{\varepsilon_{i+1}(f)} \cos\theta_{i+1} / \sqrt{\varepsilon_i(f)} \cos\theta_i}{1 + \sqrt{\varepsilon_{i+1}(f)} \cos\theta_{i+1} / \sqrt{\varepsilon_i(f)} \cos\theta_i} \quad t_{v(i-1)}(f) = \frac{2}{1 + \sqrt{\varepsilon_i(f)} \cos\theta_i / \sqrt{\varepsilon_{i-1}(f)} \cos\theta_{i-1}} \quad (2)$$

where  $\varepsilon_i(f)$  is the complex form of the permittivity and the suffix  $i$ ,  $i - 1$  and  $i + 1$  denote current, preceding and succeeding layers respectively. The incident polarized electric field is assumed to be propagating in the  $x$ -direction normal to the interface:

$$E_{yi}(x, t) = E_0 \times e^{i(2\pi ft - k_i x)} \quad (3)$$

$$H_{zi}(x, t) = \sqrt{\mu_1(f)\varepsilon_1(f)} E_0 \times e^{i(2\pi ft - k_i x)} \quad (4)$$

The arterial layer is layer 1, the stent layer 2, and the blood layer 3. At the interface from air to layer1, the electric field is parallel to the interface. The transmitted and reflected components of the electric and magnetic fields through layer 2 are:

$$E_{th2}(x, t) = t_{h1}(f) E_0 e^{-\delta_1(f) \frac{\Delta x_1}{2} + i(2\pi ft - k_2 x)} \quad (5)$$

$$E_{rh2}(x, t) = t_{h1}(f) r_{h2}(f) E_0 e^{-\delta_1(f) \frac{\Delta x_1}{2} - \delta_2(f) \frac{\Delta x_2}{2} + i(2\pi ft + k_2 x)} \quad (6)$$

$$H_{th2}(x, t) = t_{h1}(f) \sqrt{\mu_2(f)\varepsilon_2(f)} E_0 \sin(\theta_{r2}) e^{-\delta_1(f) \frac{\Delta x_1}{2} + i(2\pi ft - k_2 x)} \quad (7)$$

$$H_{rh2}(x, t) = t_{v1}(f) r_{v2}(f) \sqrt{\mu_2(f)\varepsilon_2(f)} E_0 \sin(\theta_{r2}) e^{-\delta_1(f) \frac{\Delta x_1}{2} - \delta_2(f) \frac{\Delta x_2}{2} + i(2\pi ft + k_2 x)} \quad (8)$$

Where  $\delta_1(f)$  and  $\delta_2(f)$  are the absorption coefficients of respective media and  $k_2(f)$  is its wavenumber.